Available online at www.sciencedirect.com
SCIENCE DIRECT®
Journal of Solid State Chemistry 178 (2005) 1630–1636
JOURNAL OF SOLID STATE CHEMISTRY
www.elsevier.com/locate/jssc

$S^+X^-I^+$ route to mesostructured materials from Fau and Beta zeolite precursors: A comparative study of their assembly behaviors in extremely acidic media

Junlin Zheng*, Shangru Zhai, Dong Wu, Yuhan Sun

State Key Laboratory of Coal Conversion, Institute of Coal Chemistry, Chinese Academy of Sciences, P.O. Box 165, Taiyuan 030001, PR China

Received 19 December 2004; received in revised form 28 February 2005; accepted 6 March 2005

Abstract

Mesoporous molecular sieves were synthesized from Beta and Fau zeolite precursors through $S^+X^-I^+$ route under extremely acidic conditions in parallel (designated as M_{Beta} and M_{Fau}, respectively). The textural properties of M_{Fau} were different from its M_{Beta} counterpart but resembled normal MCM-41 silica from TEOS. Al content in M_{Beta} was almost equivalent to that in the initial Beta zeolite precursors, whereas only trace Al species was present in M_{Fau} from elemental analysis results. The hydrothermal stability of M_{Beta} after post-synthesis ammonia treatment was considerably improved compared with normal MCM-41 aluminosilicates, whereas the M_{Fau} after the same procedure was as unstable as normal MCM-41 silica. Thus, the assembly behaviors of Beta and Fau zeolite precursors were comparatively studied based on these results. The microstructure of Fau zeolite precursors were degraded by the extremely acidic condition, and Al species was dissolved into the synthesis mixture. However, Beta zeolite precursors survived the chemical attack of extremely acidic media and were incorporated into mesostructured framework as primary building units.

Keywords: Mesoporous molecular sieves; Zeolite precursors; Hydrothermal stability

1. Introduction

Since the exciting discovery of M41S mesoporous molecular sieves by Mobil in 1992 [1,2], great efforts have been devoted to their practical applications as sorbents, catalysts and catalyst supports [3,4]. To overcome the disadvantages of mesoporous aluminosilicates in comparison to microporous zeolites, many approaches have been exploited to modestly improve their hydrothermal stability [5–7]. Recently, the significant improvement of hydrothermal stability has been resulted from the surfactant-assisted assembly of so-called zeolite precursors into aluminosilicate mesostructures [8]. The protozeolitic nanoclusters in the precursor solution promote zeolite nucleation by adopting AlO_4 and SiO_4 connectivities that resemble the secondary building units of a crystalline zeolite. In this regard, hydrothermally stable MCM-41 analogues have been fabricated from Fau, Beta, and MFI zeolite precursors in alkaline media (pH > 9) [9–11]. In addition, hydrothermally stable mesoporous aluminosilicates with hollow tubular morphology and hexagonal nanochannels were also prepared via the controlled coassembly of zeolite precursors and soluble silica species under basic conditions [12]. In an effort to produce hydrothermally stable mesostructures with pore sizes larger than MCM-41-type materials, mesostructured cellular foams (MCF) and very large pore SBA-15 analogues were obtained from Beta, MFI, and Fau zeolite precursors in acidic media where triblock copolymers served as templates [13–15]. These results indicated that the Beta and MFI zeolite precursors, which formed initially under basic conditions (pH > 7), could survive the extremely acidic

*Corresponding author. Fax: +86 351 404 1153.
E-mail address: mesozheng@hotmail.com (J. Zheng).

0022-4596/$ - see front matter © 2005 Elsevier Inc. All rights reserved.
doi:10.1016/j.jssc.2005.03.002

conditions (pH < 0) needed to assemble high-quality foams and large-pore hexagonal mesostructures, and the Na^+-nucleated Fau zeolite precursors also could remain intact in soft acidic media (4.5 < pH < 6.5). However, the assembly behaviors of Fau zeolite precursors under pH < 0 or even stronger acidic media have never been reported and deserve further examination.

The $S^+X^-I^+$ (where X^- is Cl^-, Br^-, NO_3^-) pathway is an important route to synthesize mesoporous molecular sieves in extremely acidic media, and the surfactant (S^+)/silicate (I^+) interaction is weaker in contrast to that in the S^+I^- route [16]. To our best, the assembly behaviours of zeolite precursors in this particular route have not been examined. If protozeolitic nanoclusters in zeolite precursors survived the extremely acidic media, different from non-preformed aluminosilicate species in the conventional synthesis of MCM-41, the larger volume and stronger rigidity of these nanoclusters would make it relatively difficult to assemble with the CTAB micelles and result in notable disorder because of weaker surfactant/silicate interactions ($S^+X^-I^+$) [17–19]. On the other hand, if the protozeolitic nanoclusters were decomposed into dissolved silicate and aluminates species in strongly acidic media, the obtained materials would resemble normal MCM-41 silica through $S^+X^-I^+$ route. Hence, the microstructural stability of zeolite precursors in extremely acidic media can be assessed according to the physicochemical properties of the resultant mesostructures synthesized from corresponding zeolite precursors. Herein, the diverse assembly behaviors of Fau and Beta zeolite precursors under extremely acidic media in $S^+X^-I^+$ route were comparatively studied on the basis of different textural characters, hydrothermal stability, and elemental compositions.

2. Experimental

2.1. Synthesis

2.1.1. Mesoporous materials from Beta zeolite precursors

The typical procedure is as follows: (1) 0.3 g sodium aluminates, 0.16 g sodium hydroxide and 4.8 g fumed silica were added into 25 mL tetraethylammonium hydroxide (TEAOH 20 wt%) solution. The mixture was transferred into a Teflon-lined stainless steel autoclave and heated to 413 K for 4 h to yield Beta aluminosilicate precursors (Si/Al = 30). (2) The precursor solution was added dropwise into 200 mL hydrochloric acid solution (2 M) containing 3.54 g cetyltrimethylammonium bromides (CTAB). After the mixture was stirred at room temperature for 1 h, the solid products were filtered, dried and calcined in air at 823 K for 6 h (designated as M_{Beta}). (3) For samples subject to further post-synthesis ammonia treatment, 1 g dried precipitates were added into 50 mL ammonia solution (1 M), loaded into a sealed autoclave and heated to 383 K for 48 h. (4) The final products were filtered, washed thoroughly, dried and calcined in air at 823 K for 6 h (designated as M_{Beta}−A). Hydrothermal stability of the fabricated M_{Beta}−A was evaluated by treatment in boiling water for 120 h.

2.1.2. Mesoporous materials from Fau zeolite precursors

The typical procedure is as follows: (1) Fau zeolite precursors (Si/Al = 9) were prepared by reacting 17.7778 g sodium silicates (27% SiO_2, 14% NaOH), 1.0543 g sodium aluminates, and 0.3129 g NaOH in determined amount of H_2O at 100 °C for 12 h [9]. (2) The mesoporous materials from Fau zeolite precursors were synthesized according to the procedures described in Section 2.1.1 with the substitution of Beta zeolite precursors. The calcined products without and with post-synthesis ammonia treatment are designated as M_{Fau} and M_{Fau}−A, respectively. Hydrothermal stability of the fabricated M_{Fau}−A was evaluated by age in boiling water for 8 h.

2.1.3. Normal MCM-41 silica from TEOS

Conventional pure silica MCM-41 was synthesized according to the literature from tetraethyl orthosilicates (TEOS) [20], the product was also filtered and washed with deionized water and dried in air. The calcined sample is nominated as M_{TEOS}.

2.2. Characterization of materials

The X-ray diffraction (XRD) patterns of the samples were recorded using a Shimadzu XD-3A X-ray powder diffractometer, which employed Ni-filtered Cu$K\alpha$ radiation and was operated at 40 kV and 30 mA. The nitrogen sorption isotherms at 77 K were measured using a Micromeritics Tristar 3000 system. The mesostructures were analyzed from desorption branches of the isotherms by the Barrett–Joyner–Halenda (BJH) model with Halsey equation for multiplayer thickness. ^{27}Al NMR spectra were recorded on a Bruker MSL-400 spectrometer, and the chemical shifts were referenced to $Al(OH)_6^{3+}$. Element analyses were operated on an Atom Scan 16 AES-ICP system to obtain the Si, Al, and Na contents.

3. Results and discussions

3.1. Textural properties

Fig. 1(A) shows the XRD patterns of M_{Fau} and M_{Beta}. Clearly, the product from Fau precursors (*a*, M_{Fau}) has (100) and (110) diffraction peaks, typical of MCM-41-type hexagonal mesostructures with good

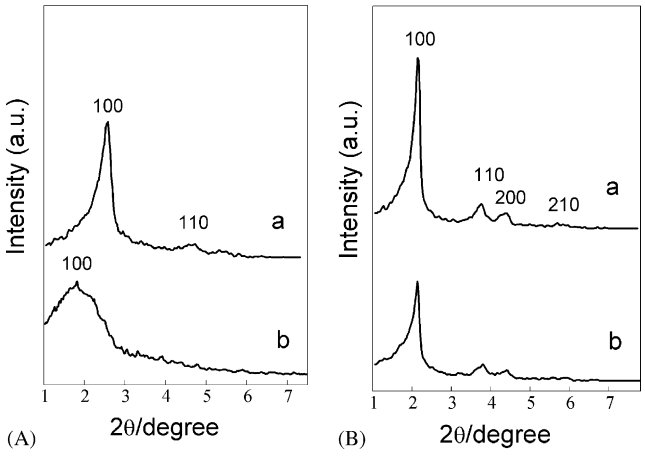

Fig. 1. XRD patterns of the mesostructured materials from Fau (a) and Beta (b) zeolite precursors: (A) as-synthesized and calcined, (B) post-synthesis ammonia treated and calcined.

long-range order. In contrast, the sample from Beta precursors (*b*, M_{Beta}) only exhibits a broad (100) diffraction peak, indicating the presence of poorly ordered mesostructure. It has been reported that post-synthesis ammonia treatment could refine the structural order and pore size uniformity of the acid-made mesoporous silica [21]. After post-synthesis treated in ammonia solution, the structural orders of both samples (M_{Beta}−*A* and M_{Fau}−*A*, respectively) are improved considerably evidenced by the XRD patterns as shown in Fig. 1(B). For the M_{Fau}−*A* sample, additional (200) and (210) diffraction peaks appear and the intensity of (100) and (110) peaks is notably enhanced (a). At the same time, for the M_{Beta}−*A* sample, the basal (100) peak become intense, meanwhile, additional (110) and (200) peaks emerge.

Fig. 2 gives the N_2 sorption isotherms and corresponding pore size distribution plots (inset) of M_{Fau} (A) and M_{Beta} (B). Obviously, both isotherms are type IV according to IUPAC classification. In Fig. 2(A), a steep increase occurs in the isotherm curve at the relative pressure of $0.30<p/p_o<0.40$, indicating the presence of highly regular mesostructures. The derived pore size distribution plot reveals a narrow 2.50 nm pore. At higher p/p_o range (>0.85), the isotherm remains flat and no hysteresis loop can be found. In contrast, a slow increase occurs in the isotherm curve (Fig. 2(B)) at the relative pressure of $0.35<p/p_o<0.45$, which can be attributed to the presence of less-ordered mesostructures. The derived pore size distribution plot implies a broad 3.06 nm pore. The second condensation step on the isotherm at $p/p_o>0.85$ indicates the presence of a significant amount of textural porosity. It can be deduced that the particle size of M_{Fau} was much larger than that of M_{Beta}.

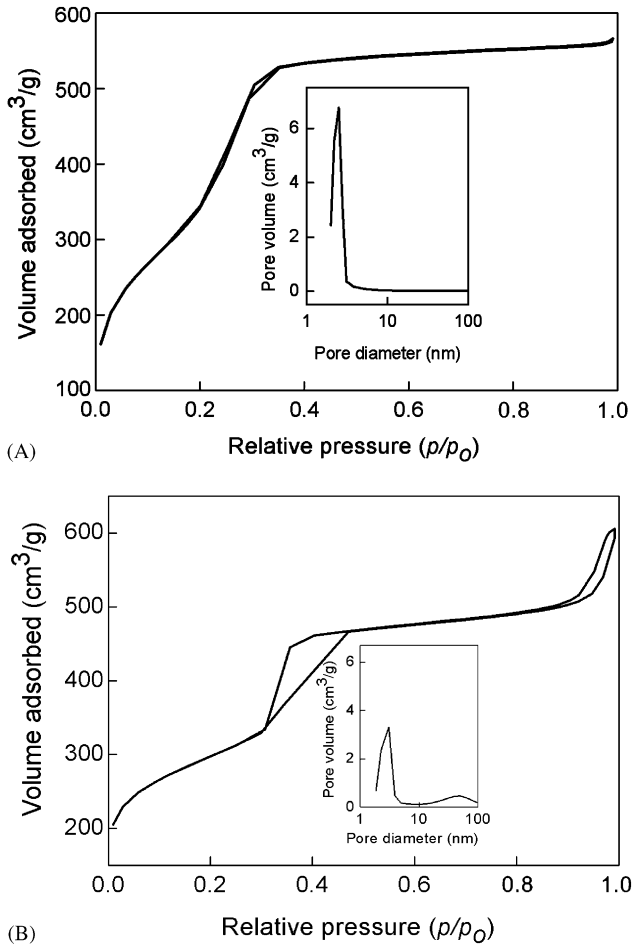

Fig. 2. N_2 sorption isotherms and pore size distribution plots (inset) of the mesostructured M_{Fau} (A) and M_{Beta} (B).

Pure MCM-41 silica (M_{TEOS}) was prepared for comparison using TEOS as silica sources and cationic surfactant CTAB as the template through the same $S^+X^-I^+$ route. The presence of (100), (110) and (200) diffraction peaks in XRD pattern, as shown in Fig. 3(A), confirms the presence of high-quality mesostructures. The N_2 sorption isotherms (Fig. 3(B)) of M_{TEOS} are in agreement with the XRD results. A steep increase occurs in the type IV isotherm curve at the relative pressure of $0.30<p/p_o<0.40$, and the derived pore size distribution plot shows a narrow 2.48 nm pore. Interestingly, the textural properties of M_{TEOS}, including d_{100}, pore diameter, wall thickness, BET surface areas, and pore volumes, are completely comparable to those of M_{Fau}.

From XRD and N_2 sorption results, the textural properties of so-produced samples are given in Table 1. The d_{100} values of M_{Beta} and M_{Fau} are 4.78 and 3.39 nm, and the d_{100} values shift to 4.15 and 4.11 nm after post-synthesis ammonia treatment, respectively. The pore diameters of M_{Beta} and M_{Fau} change from 3.06, 2.50 to 2.75, 2.73 nm, and the wall thickness shift from 2.46, 1.41 to 2.04, 2.02 nm, respectively. The changes of d_{100}

value, pore diameter, and wall thickness fall into the opposite trends for M_{Beta} and M_{Fau} mesostructures. The BET surface areas and pore volumes of M_{Beta} decrease sharply, whereas those of M_{Fau} show no remarkable change after post-synthesis ammonia treatment. Although both M_{Beta} and M_{Fau} are fabricated from zeolite precursors through $S^+X^-I^+$ route under extremely acidic conditions, their textural properties and their transformation trends via post-synthesis ammonia treatment procedure are notably different.

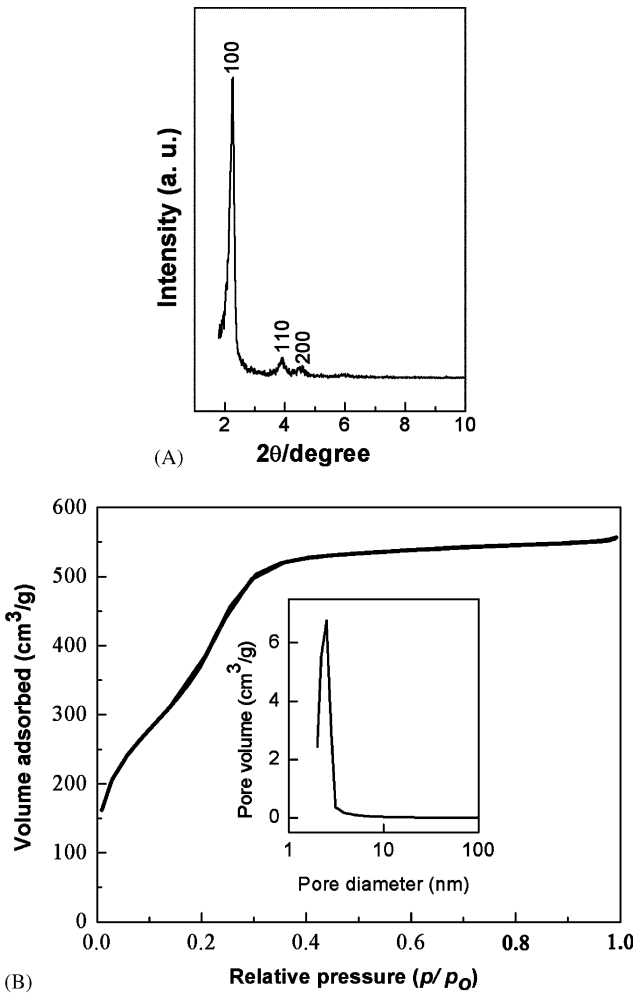

Fig. 3. XRD (A) and N_2 sorption isotherm (B pore size distribution plot inset) of M_{TEOS}.

3.2. Hydrothermal stability test

As discussed in the previous literatures [13,14], mesoporous molecular sieves from both Fau and Beta zeolite precursors (in proper pH range) possess improved hydrothermal stability, which may be attributed to the incorporation of zeolite subunits into the framework walls of the resultant mesostructures [8]. $M_{Beta}-A$ and $M_{Fau}-A$ samples were aged in boiling water to validate whether their hydrothermal stabilities had considerable improvement or not in this particular route. Fig. 4 shows the XRD patterns of $M_{Fau}-A$ (a) and $M_{Beta}-A$ (b) samples after aged in boiling water. Clearly, well-resolved (100), (110), (200), and (210) diffraction peaks of $M_{Fau}-A$, which indicating high-quality mesostructures, disappear completely merely after 8 h age. In contrast, the (100), (110), and (200) diffraction peaks of the $M_{Beta}-A$ are still present even after 120 h age in boiling water. Mesoporous materials from Beta zeolite precursors show remarkably improved hydrothermal stability, and the zeolite primary building units introduced into the mesostructured frameworks are responsible for the improved hydrothermal stability [19]. Contrastively, unlike $M_{Beta}-A$ with improved hydrothermal stability, $M_{Fau}-A$ exhibits unexpectedly poor hydrothermal stability even lower than normal MCM-41 aluminosilicates. The hydrothermal stability of $M_{Fau}-A$ is just as poor as normal MCM-41 silica.

3.3. Element analysis results

Acid leaching treatment is well known to cause dealumination of zeolite aluminosilicates, that is, removal of aluminum atoms from the aluminosilicate framework [22–24]. Zeolite precursors comprise abundant protozeolitic nanoclusters that nucleate zeolite as primary and secondary building units. Considering their vulnerability, the dealumination effect of Fau and Beta protozeolitic nanoclusters in extremely acidic media might be more violent. Therefore, element analysis is applied to determine how much the Al species present in zeolite precursors has been incorporated into resultant mesostructures. Table 2 gives the element analysis data. The percentages of Si, Al, and Na elements in the resultant M_{Beta} are 44.03%, 1.29%, and

Table 1
Textural properties of the mesostructured materials from Beta, Fau zeolite precursors and TEOS

Samples	d_{100}/nm	Pore diameter/nm	Wall thickness/nm	S_{BET}/$m^2 g^{-1}$	Pore volume/$cm^3 g^{-1}$
M_{Beta}	4.78	3.06	2.46	914	0.98
$M_{Beta}-A$	4.15	2.75	2.04	663	0.62
M_{Fau}	3.39	2.50	1.41	1274	0.86
$M_{Fau}-A$	4.11	2.73	2.02	1047	0.88
M_{TEOS}	3.34	2.48	1.38	1428	0.85

0.09%, respectively. The Si/Al molar ratio is 32.29, which is slightly higher than that of Beta zeolite precursors. In contrast, the percentages of Si, Al, and Na elements in the resultant M_{Fau} are 45.92%, 0.0026%, and 0.001%, respectively. Only trace Al elements enter into the framework of M_{Fau}. The ^{27}Al MAS NMR (Fig. 5) of M_{Beta} (b) exhibits chemical shifts at 56 and 0 ppm assigned to 4- and 6-coordinated Al, respectively, whereas no Al signals were detected in the M_{Fau} (a) sample. These results clearly show that most Al species have been tetrahedrally incorporated into the framework of M_{Beta} despite the extremely acidic conditions. It has been reported that MSU-S could be fabricated with cationic surfactants acting as templates under pH = 9

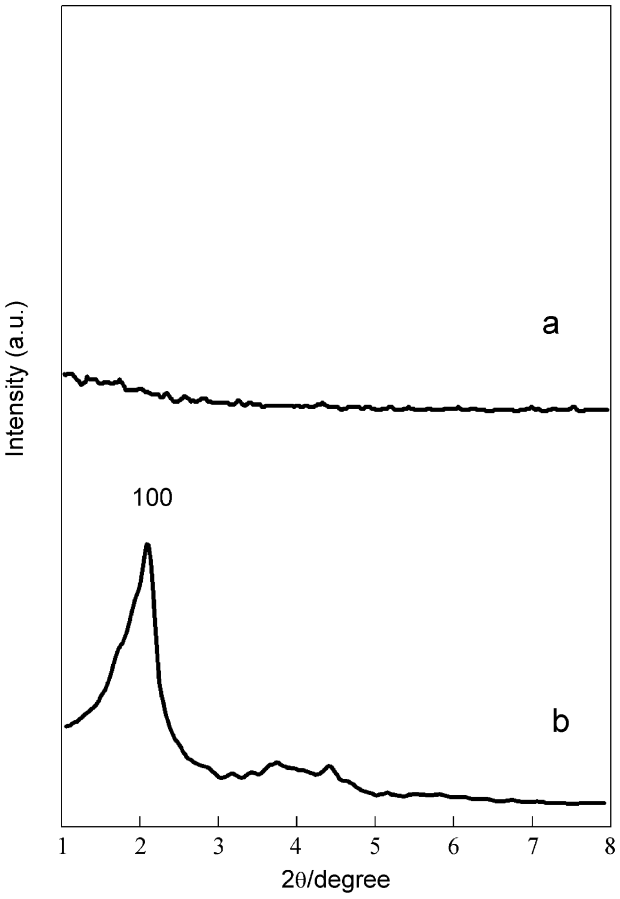

Fig. 4. XRD patterns of the mesostructured materials: (a) M_{Fau}–A aged for 8 h (b) M_{Beta}–A aged for 120 h in boiling water.

Table 2
Element analysis results of the mesostructured materials from Beta and Fau zeolite precursors

	Si % (wt)	Al % (wt)	Na % (wt)	Si/Al (molar ratio)
M_{Beta}	44.03	1.29	0.090	32.91
M_{Fau}	45.92	0.0026	0.0010	~17000

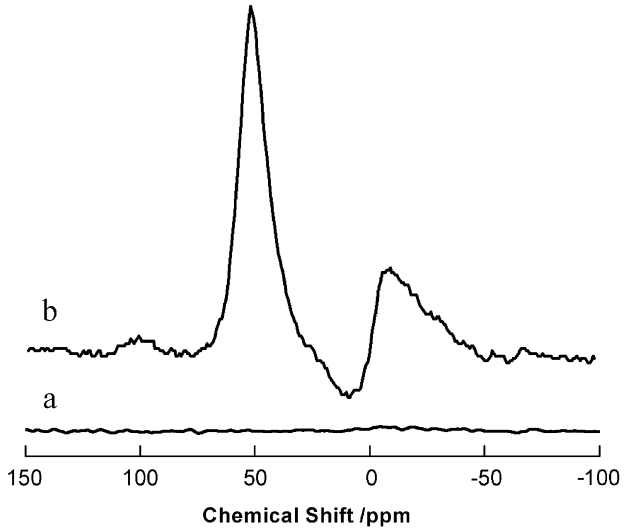

Fig. 5. ^{27}Al MAS NMR of mesostructured M_{Fau} (a) and M_{Beta} (b).

and MSU-S/F_{Fau} could be synthesized with non-ionic surfactants served as templates under pH = 4.5–6.5, and both samples exhibited resolved ^{27}Al MAS NMR spectra equivalent to that of the initial Fau zeolite precursors [9,13]. Combined with reported results, although Al species present in Fau precursor solution could be incorporated into mesostructured frameworks in alkaline or weak acidic media, most of Al species was dissolved during the assembly process under present rigorous acidic media.

Fau zeolite precursors were produced from sodium aluminates, sodium hydroxide, and sodium silicates (~1.82 g Na elements in it), and Beta zeolite precursors were prepared from sodium aluminates, sodium hydroxide, and fumed silica (~0.15 g Na elements in it) in the current procedures. The absolute majority of Na elements in Beta zeolite precursors remained in the extremely acidic media. Although Na^+ involved in the synthesis of Fau zeolite precursors was much higher than that in the formation of Beta zeolite precursors, M_{Beta} was ninety times higher than M_{Fau} in Na content after the assembly process in extremely acidic media.

3.4. Different assembly behaviors

As described above, the mesostructured materials from Fau and Beta zeolite precursors have diverse textural characters, hydrothermal stability, and elemental compositions. In this section, the assembly behavior of Fau and Beta zeolite precursors in current route will be discussed briefly to explain the phenomena. The mesostructures of M_{Beta} are poorly ordered, and the hydrothermal stability of M_{Beta}–A is notably improved compared to traditional MCM-41 aluminosilicates. Furthermore, most Al species has been tetrahedrally

incorporated into the framework of M_{Beta} despite the extremely acidic conditions. So it can be concluded that Beta zeolite precursors survive the extremely acidic media and are incorporated into mesostructured framework as primary building units. Or else, if the protozeolitic nanoclusters were degraded in the extremely acidic media, Al species in the form of Al^{3+} would remain in the strongly acidic solution and there should be no tetrahedral Al signal present in the ^{27}Al NMR spectra of M_{Beta}. It is proposed that the reserved zeolite-like connectivity of tetrahedral SiO_4 and AlO_4 units upon assembling the nanoclusters into mesostructured materials plays a very important role in the improvement of hydrothermal stability [8,25]. Considering the weak surfactant/silicate interaction in $S^+X^-I^+$ route and larger volume of Beta protozeolitic nanoclusters, the increase of d_{100} space value and pore wall thickness, decrease in structural order, and formation of textural mesoporosity can also be well explained by the integrity of Beta protozeolitic nanoclusters. The textural properties of M_{Fau} resemble normal MCM-41 silica from TEOS through $S^+X^-I^+$ route, and M_{Fau} are born with resolved mesostructures; the hydrothermal stability of $M_{Fau}-A$ is as poor as normal MCM-41 silica; trace Al species can be detected in mesostructured M_{Fau}. As to the Fau zeolite precursors, the protozeolitic nanoclusters in it collapse into dissolved silicate and aluminate species in the extremely acidic media ($pH<0$). Al elements in the form of Al^{3+} remain in the synthesis system. The mesostructures of M_{Fau} based on dissolved silicate species are deservedly highly ordered, and the hydrothermal stability equal to normal MCM-41 silica can also be fully explained [26]. The lower d_{100} space value and pore wall thickness can be attributed to the shrinkage of poorly polymerized pure silica framework during calcination. Thus, the higher hydrothermal stability of $M_{Beta}-A$ than $M_{Fau}-A$ is not only due to the incorporation of pre-zeolitic units but also to the presence of Al element in the framework wall of $M_{Beta}-A$ [27,28].

Much more Na^+ elements are present in M_{Beta} mesostructures than in M_{Fau} in spite of largely higher dosage of Na^+ in the starting materials. The alteration of sodium contents in the synthesis process of M_{Fau} can also verify the degradation of Fau zeolite precursors. It has been shown that hydrated Na^+ cation played an important role in the nucleation of Y zeolite. Broad line ^{23}Na NMR technique has been applied to investigate the formation of Fau zeolite precursors and growth of these precursors. When the original Na_2O–Al_2O_3–SiO_2–H_2O system was in gel state, ^{23}Na NMR could not find the spectrum of these disordered Na^+. After Fau zeolite precursors formed in the gel system, Na^+ combined with the protozeolitic nanoclusters, and ^{23}Na NMR can observe the spectrum of ordered Na^+ in zeolite structure [29]. It has been well established that dealumination with acids was accompanied by ion exchange of lattice Na^+ cation by protons. Almost all the Na elements escaped from Fau zeolitic precursors in extremely acidic media from element analysis. Considering the unexpectedly low Al and Na contents in the final M_{Fau}, it is clear that the microstructures of Fau zeolite precursors were totally destroyed and were reduced into dissolved silicates and aluminates in the extremely acidic media. Most of Na and Al elements remained in the filtrate.

Based on parallel hydrothermal stability test and element analysis, it is deduced that the stability of Fau zeolite precursors is relatively poorer than Beta zeolite precursors in extremely acidic media with the same concentration. The phenomena may probably be explained on the following aspects: (1) TEA^+ organic cation serving as templates stabilize Beta zeolite precursors against acid attack, while dehydrated Na^+ cation are vulnerable to the extremely acidic environments; (2) Beta zeolite is intrinsically more stable than Y zeolite against acid leaching [30]. Thus, their primary structural units may obey the same stability order in extremely acidic media.

4. Conclusions

The assembly behaviors of Fau and Beta zeolite precursors in extremely acidic media were comparatively investigated via current $S^+X^-I^+$ pathway based on their diverse textural properties, hydrothermal stability, and elemental compositions. Beta zeolite precursors survived the extremely acidic media and were incorporated into mesostructured framework as primary building units. However, the microstructure of Fau protozeolitic nanoclusters collapsed in the extremely acidic media, and Al, Na species were dissolved into the synthesis mixture. The stability of Fau zeolite precursors is relatively poorer than Beta zeolite precursors in extremely acidic media.

Acknowledgments

Financial supports from National Key Basic Research Special Foundation (G2000048001) are gratefully acknowledged.

References

[1] C.T. Kresge, M.E. Leonowicz, W.J. Roth, J.C. Vartuli, J.S. Beck, Nature 359 (1992) 710.
[2] J.S. Beck, J.C. Vartuli, W.J. Roth, M.E. Leonowicz, C.T. Kresge, K.O. Schmitt, C.T.-W. Chu, D.H. Olson, E.W. Sheppard, S.B. McCullen, J.B. Higgins, J.L. Schlenker, J. Am. Chem. Soc. 114 (1992) 10834.

[3] A. Corma, V. Fornes, M.T. Navarro, J. Perez-Pariente, J. Catal. 148 (1994) 569.
[4] A. Corma, Chem. Rev. 197 (1997) 2373.
[5] D. Das, C.M. Tsai, S. Cheng, Chem. Commun. (1999) 473.
[6] J.M. Kim, S. Jun, R. Ryoo, J. Phys. Chem. B 103 (1999) 6200.
[7] R. Mokaya, J. Phys. Chem. B 103 (1999) 10204.
[8] Y. Liu, T.J. Pinnavaia, J. Mater. Chem. 12 (2002) 3179.
[9] Y. Liu, W.Z. Zhang, T.J. Pinnavaia, J. Am. Chem. Soc. 122 (2000) 8791.
[10] Z.T. Zhang, Y. Han, F.-S. Xiao, S.L. Qiu, L. Zhu, R.W. Wang, Y. Yu, Z. Zhang, B.S. Zou, Y.Q. Wang, H.P. Sun, D.Y. Zhao, Y. Wei, J. Am. Chem. Soc. 123 (2001) 5014.
[11] Y. Liu, W.Z. Zhang, T.J. Pinnavaia, Angew. Chem. Int. Ed. 40 (2001) 1255.
[12] J.L. Zheng, Y. Zhang, Z.H. Li, W. Wei, D. Wu, Y.H. Sun, Chem. Phys. Lett. 376 (2003) 136.
[13] Y. Liu, T.J. Pinnavaia, Chem. Mater. 14 (2002) 3.
[14] Y. Han, F.-S. Xiao, S. Wu, Y.Y. Sun, X.J. Meng, D.S. Li, S. Li, J. Phys. Chem. B 105 (2001) 7963.
[15] Y. Han, S. Wu, Y.Y. Sun, D.S. Li, F.-S. Xiao, J. Liu, X.Z. Zhang, Chem. Mater. 14 (2002) 1144.
[16] Q.S. Huo, D.I. Margolese, U. Clesia, P.Y. Feng, T.E. Gler, P. Sleger, R. Leon, P.M. Petroff, F. Schuth, G.D. Stucky, Nature 368 (1994) 24.
[17] P.-P.E.A. de Moor, T.P.M. Beelen, R.A. van Santen, K. Tsuji, M.E. Davis, Chem. Mater. 11 (1999) 36.
[18] D.P. Serrano, R. van Grieken, J. Mater. Chem. 11 (2001) 2391.
[19] J.L. Zheng, Y. Zhang, D. Wu, Y.H. Sun, Acta Phys.-Chim. Sin. 19 (2003) 907.
[20] Q.S. Huo, D.I. Margolese, U. Clesia, P.Y. Feng, T.E. Gler, P. Sleger, R. Leon, P.M. Petroff, F. Schuth, G.D. Stucky, Nature 368 (1994) 24.
[21] H.P. Lin, C.Y. Mou, S.B. Liu, C.Y. Tang, C.Y. Lin, Micropor. Mesopor. Mater. 44–45 (2001) 129.
[22] M.R. Apelian, A.S. Fung, G.J. Kennedy, T.F. Degnan, J. Phys. Chem. 100 (1996) 16577.
[23] T.E. White, R.A. Dalla Betta, E.G. Derouane, R.T.K. Baker, (Eds.), Catalytic Materials: Relationship Between Structure and Reactivity, ACS Symposium Series, American Chemical Society, Washington, DC, 1984, 385pp.
[24] H. Stach, U. Lohse, H. Thamm, W. Schirmer, Zeolites 6 (1986) 74.
[25] T.R. Pauly, V. Petkov, Y. Liu, S.J.L. Billinge, T.J. Pinnavaia, J. Am. Chem. Soc. 124 (2002) 97.
[26] Y. Han, N. Li, L. Zhao, D.F. Li, X.Z. Xu, S. Wu, Y. Di, C.J. Li, Y.C. Zou, Y. Yu, F.-S. Xiao, J. Phys. Chem. B 107 (2003) 7551.
[27] Y.D. Xia, R. Mokaya, Micropor. Mesopor. Mater. 74 (2004) 179.
[28] A.S. O'Neil, R. Mokaya, M. Poliakoff, J. Am. Chem. Soc. 124 (2002) 10636.
[29] R.R. Xu, J.M. Zhang, Chem. J. Chinese Univ. 3 (1982) 287.
[30] J.P. Shen, Y. Li, T. Sun, J. Guo, B. Zhang, D.Z. Jiang, E.Z. Min, T.S. Jiang, Chem. J. Chinese Univ. 16 (1995) 943.